

DTIC FILE COPY

5

MEMORANDUM REPORT BRL-MR-3715

BRL

1938 - Serving the Army for Fifty Years - 1988

AD-A201 713

TECHNIQUES FOR THE MEASUREMENT
OF TANK CANNON JUMP

JONATHAN BORNSTEIN
ILMARS CELMINS
PETER PLOSTINS
E. M. SCHMIDT

DECEMBER 1988

Best Available Copy

S DTIC ELECTE **D**
DEC 27 1988
E

APPROVED FOR PUBLIC RELEASE; DISTRIBUTION UNLIMITED

U.S. ARMY LABORATORY COMMAND

**BALLISTIC RESEARCH LABORATORY
ABERDEEN PROVING GROUND, MARYLAND**

88 12 27 008

UNCLASSIFIED

SECURITY CLASSIFICATION OF THIS PAGE

REPORT DOCUMENTATION PAGE				Form Approved OMB No. 0704-0188		
1a. REPORT SECURITY CLASSIFICATION UNCLASSIFIED			1b. RESTRICTIVE MARKINGS			
2a. SECURITY CLASSIFICATION AUTHORITY		3. DISTRIBUTION / AVAILABILITY OF REPORT				
2b. DECLASSIFICATION / DOWNGRADING SCHEDULE		Approved for public release; distribution unlimited				
4. PERFORMING ORGANIZATION REPORT NUMBER(S) bRL-MR-3715			5. MONITORING ORGANIZATION REPORT NUMBER(S)			
6a. NAME OF PERFORMING ORGANIZATION U.S. Army Ballistic Research Laboratory		6b. OFFICE SYMBOL (if applicable) SLCBR-LF	7a. NAME OF MONITORING ORGANIZATION			
6c. ADDRESS (City, State, and ZIP Code) Aberdeen Proving Ground, MD 21005-5066			7b. ADDRESS (City, State, and ZIP Code)			
8a. NAME OF FUNDING / SPONSORING ORGANIZATION U.S. Army Ballistic Research Laboratory		8b. OFFICE SYMBOL (if applicable) SLCBR-DM-T	9. PROCUREMENT INSTRUMENT IDENTIFICATION NUMBER			
8c. ADDRESS (City, State, and ZIP Code) Aberdeen Proving Ground, MD 21005-5066			10. SOURCE OF FUNDING NUMBERS			
			PROGRAM ELEMENT NO. 62618A	PROJECT NO. 62618AH80	TASK NO. 1L1	WORK UNIT ACCESSION NO.
11. TITLE (include Security Classification) TECHNIQUES FOR THE MEASUREMENT OF TANK CANNON JUMP (U)						
12. PERSONAL AUTHOR(S) Bornstein, Jonathan, Gelmins, Ilmars, Plostins, Peter, and Schmidt, E.M.						
13a. TYPE OF REPORT Memorandum Report		13b. TIME COVERED FROM 5-85 TO 2-88	14. DATE OF REPORT (Year, Month, Day) 1988 September		15. PAGE COUNT 30	
16. SUPPLEMENTARY NOTATION						
17. COSATI CODES			18. SUBJECT TERMS (Continue on reverse if necessary and identify by block number)			
FIELD	GROUP	SUB-GROUP	Instrumentation			
19	6		M256			
14	2		120mm			
			Tank Gun			
			Gun Dynamics			
			Jump			
19. ABSTRACT (Continue on reverse if necessary and identify by block number)						
<p>→ To attain the goal of producing tank main gun systems possessing enhanced accuracy, an experimental methodology examining the disturbances acting upon a projectile during the launch process and initial stages of free flight has been developed. The disturbances are characterized by the angular deviation of the projectile trajectory from an anticipated line of flight extending between the gun muzzle and the aim point prior to firing the cannon. Gun motion during the projectile in-bore time, including both rotation of the tube about the trunnions and vibrations of the cannon, is determined using a combination of strain gauges and proximity probes. This information provides the orientation of the muzzle relative to the line of fire and gun velocity perpendicular to the projectile line of flight at the instant the bullet leaves the cannon. A technique employing multiple orthogonal x-rays is used to measure both the linear c.g. and angular motion of the projectile during the transitional</p> <p style="text-align: right;">(continued)</p>						
20. DISTRIBUTION / AVAILABILITY OF ABSTRACT <input type="checkbox"/> UNCLASSIFIED/UNLIMITED <input checked="" type="checkbox"/> SAME AS RPT <input type="checkbox"/> DTIC USERS			21. ABSTRACT SECURITY CLASSIFICATION UNCLASSIFIED			
22a. NAME OF RESPONSIBLE INDIVIDUAL Dr. Jonathan A. Bornstein		22b. TELEPHONE (include Area Code) (301)-278-3737		22c. OFFICE SYMBOL SLCBR-IF-F		

DD Form 1473, JUN 86

Previous editions are obsolete.

SECURITY CLASSIFICATION OF THIS PAGE

UNCLASSIFIED

UNCLASSIFIED

19. ABSTRACT (continued)

ballistic flight phase. Radiographs taken in the immediate vicinity of the muzzle provide the initial flight dynamics, indicating the relative motion of the projectile with respect to the muzzle caused by in-bore balloting, gun/projectile decoupling, initial sabot discard and muzzle blast disturbances. Comparison of these measurements with those obtained from radiographs obtained after sabot separation yield a quantitative measure of the disturbances due to asymmetric sabot discard. The measurements also provide the initial conditions for the free flight trajectory of the projectile. (FR)

UNCLASSIFIED

Table of Contents

	<u>Page</u>
List of Figures	v
I. Introduction	1
II. Methodology	3
III. Gun Dynamics	4
1. Proximity Probes	5
2. Strain Measurements	6
IV. Transitional Ballistics	7
V. Jump Analysis	10
VI. Concluding Remarks	11
VII. References	21
List of Symbols	23
Distribution List	25

Accession For	
NTIS GRA&I	<input checked="" type="checkbox"/>
DTIC TAB	<input type="checkbox"/>
Unannounced	<input type="checkbox"/>
Justification	
By _____	
Distribution/	
Availability Codes	
Dist	Avail and/or Special
A-1	



List of Figures

<u>Figure</u>		<u>Page</u>
1	Vector diagram indicating the closure analysis with sources of disturbance to the projectile trajectory	12
2	Schematic diagram of set-up for tests	12
3	Diagram of 120mm M256 gun tube with breech indicating the location of the proximity probes (arrows) and strain gauges (crosses) used to determine the gun dynamics	13
4	Transverse motion of the gun tube near the muzzle (TPCSDS-T projectile)	13
5	Expansion of the gun tube near the muzzle (TPCSDS-T projectile)	14
6	Muzzle pointing angle measured by proximity probes (TPCSDS-T projectile)	14
7	Sample strain record	15
8	Displacement of the tube (a) vertical plane, (b) horizontal plane	15
9	Schematic representation of x-ray set-up	16
10	TPCSDS-T projectile at launch. Muzzle is shown at left of photo. Lower image shows pitching of projectile, upper indicates yawing motion.	16
11	TPCSDS-T projectile 3 meters downrange of muzzle. Lower photo shows pitching of projectile, upper indicates yawing motion.	17
12	TPCSDS-T projectile entering free flight, 10.4 meters downrange. Lower photo shows pitching of projectile, upper indicates yawing motion.	17
13	CG trajectory of TPCSDS-T projectile - vertical plane	18
14	CG trajectory of TPCSDS-T projectile - horizontal plane	18
15	Pitch history for TPCSDS-T projectile determined from x-ray data	19
16	Yaw history for TPCSDS-T projectile determined from x-ray data	19
17	Closure diagram for TPCSDS-T projectile	20

I. Introduction

In the currently projected battlefield environment the quality of American weapon systems is pitted against the quantity possessed by opposing forces. Therefore, it is becoming increasingly important for our armor forces to possess a first round kill capability. This requirement effectively translates into the development of tank main gun systems possessing enhanced accuracy. An initial step in this direction is the quantitative determination of those disturbances which significantly affect the accuracy of tank gun ammunition, both sabot Kinetic Energy (KE) and full bore High Explosive Anti-Tank (HEAT) ammunition. Once this is accomplished, those areas in which meaningful contributions to improved accuracy can be made, may be identified.

No single quantity fully describes the accuracy of ammunition, rather one must utilize a hierarchy of values. The lowest order term in this hierarchy is the ammunition dispersion or standard deviation of a series of impacts obtained from a single gun firing a single type and lot of ammunition during a single occasion. The next rung on the ladder is the deviation of the group center of impact from the aim point for this occasion. Then consideration can be given to variation in center of impact between gun tubes and tanks. In this paper, the hierarchy is limited to a single firing wherein the angular deviation between the aim and impact points, i.e., the jump is examined in detail.

The overall jump of the projectile is the resultant of many disturbances. For purposes of illustration, consider the flight of a sabot projectile. Prior to launching the round, the gun is aimed at a target. The propellant charge is ignited and the high pressure combustion gases propel the round forward in the gun tube. The gases also exert a force upon the breech, causing it to recoil rearward in its mount. If the center of pressure is laterally offset from the center of mass of the system, this force produces a moment causing the gun tube to rotate around the trunnions. Although an idealized cannon bore is perfectly straight, gun tubes typically have some curvature due to machining, droop under gravity and firing dynamics. This results in the occurrence of interactions between the gun tube and projectile, causing a mutual exchange of transverse momentum. At the instant the projectile is launched, the muzzle therefore is no longer pointing where it was initially aimed.

The sabot kinetic energy round consists of a sub-caliber penetrator rod encased within a lightweight, elastic sabot. The combination of penetrator and sabot may be considered as a system of spring/mass elements, subjected to forces as it follows the irregular curvature of the gun. The resulting transverse motion, causes the projectile/sabot combination to ballot and vibrate giving it a linear velocity which is not aligned with the gun tube centerline and an angular velocity about its own center of gravity. Within the gun tube, the projectile/sabot is supported at two points along its length. As it exits the gun muzzle, it sequentially loses the support of these two boreriders. During the decoupling, conditions can arise which result in a force and/or moment being imparted to the bullet.

During the initial few meters of flight, the projectile flies through the muzzle blast. The bullet is subjected to abnormal ambient conditions, resulting from the outward flow of gas from the gun muzzle over the rear of the projectile. The resulting pressure distribution

on the bullet, particularly in the case of finned projectiles, can give rise to forces and moments which deflect it from its initial trajectory.

The process of sabot separation begins as the bullet leaves the gun tube. Due to the transverse motions of the projectile as it moves down the bore of the tube, energy is stored in the elastic sabot petals. As the projectile leaves the muzzle, the constraints of the gun tube are released and the sabot elements are able to move laterally outward. Aerodynamic forces acting on each of the sabot petals then causes them to lift up and physically disengage from the buttress grooves of the penetrator rod. Despite the higher drag forces acting on each petal, the sabot elements will fly in close proximity to the penetrator for several meters downrange. Aerodynamic interaction between the sabot and projectile will occur throughout this period. Asymmetric shock waves formed due to the supersonic flight of the sabot elements impinge upon the penetrator body and fins, imparting disturbances. Ultimately the sabot petals move sufficiently far from the penetrator, either to the side or rear, to prevent further interaction and the penetrator is in free flight. However in the process, both aerodynamic and mechanical disengagement asymmetries can result in a significant net force and moment being applied to the penetrator.¹ As the projectile enters free flight, it has an initial yaw angle ξ_0 and rate ξ'_0 . The net lift force acting upon the projectile as a result of the yawing motion produced by the initial rate results in a deflection of the trajectory known as aerodynamic jump. For most finned projectiles of interest, the yaw rapidly damps and the magnitude of this term can be determined from the values of C_{M_a} , C_{L_a} and ξ'_0 , as shown by Murphy.²

Lastly, the projectile is subject to both cross winds and gravity as it flies downrange. The effect of gravity is directly related to the time of flight to the target. Hence it can be determined from a knowledge of the projectile drag coefficient, initial velocity and range to the target. The influence of cross winds will be a function of the projectile geometry and the range to the target and can be minimized by limiting testing to periods when their magnitude is small. For the tests reported upon in this paper, the initial portion of the projectile trajectory was indoors, through the Transonic Range Facility, thus reducing further the impact of cross-winds upon the results.

Each of these disturbance sources has the potential to significantly affect accuracy, either the jump or the ammunition dispersion. To rationally approach the problem of maximizing accuracy, it is first necessary to quantify the contribution of each disturbance. A methodology to accomplish this task has been developed at BRL and during the past three years it has been utilized to examine the behavior of ammunition currently in the inventory for the 105 mm and 120 mm Main Guns of the M1 and M1A1 tanks. This paper will provide an overview of the test methodology and instrumentation required to measure the launch disturbances. The "closure analysis" which unifies the jump components, indicating the contribution of each to the overall jump of the projectile will also be discussed.

¹Plostins, P., "Launch Dynamics of APFSDS Ammunition". BRL Technical Report BRL-TR-2595, U.S. Army Ballistic Research Lab, Aberdeen Proving Ground, MD 21005-5066, 1984

²Murphy, C.H., "Free Flight Motion of Symmetric Missiles". BRL Technical Report 1216, U.S. Army Ballistic Research Laboratory, Aberdeen Proving Ground, MD 21005-5066, 1963

II. Methodology

To quantify the effects of various disturbance sources on projectiles, the overall jump of the bullet has been divided into component parts which can be physically measured. Figure 1 depicts the closure analysis for a typical sabot round. The analysis summarizes the contribution of the possible disturbance sources outlined in the introduction. Each disturbance is represented by a vector equal to the angular deviation of the projectile trajectory caused by the disturbance. In some instances, multiple sources act at a given point in the projectile trajectory and separation of the contributions is not possible. Under these circumstances, it is necessary to lump the deviation due to a number of disturbances into a single vector. If all the disturbances have been accurately measured, the vector summation of the individual components will be equal to the angular coordinate of the actual impact point, yielding "closure". From an analysis of the error sources associated with each of the measurement techniques, it has been concluded that under optimal circumstances the analysis is accurate to approximately 0.2 milliradians. Thus, cases for which the difference between the summation of the measured disturbances and the actual impact point is less than 0.2 milliradians will be said to exhibit closure.

Figure 2 is a sketch of the experimental set-up for the tests. All tests were conducted from a tank mounted cannon firing at a target located approximately 1 kilometer downrange. The cannon is aimed directly at the target cross using a collimated muzzle borescope and no superelevation is used to compensate for gravity drop. On the gun itself and between the muzzle and the target, a wide variety of instrumentation, some of which is shown in the diagram, has been utilized to determine both the gun dynamics and the motion of the projectile as it flies downrange.

The gun dynamics contribution to the overall jump, measured using a combination of proximity probes and strain gauges, is represented by two vectors in figure 1. The first begins at the aim point, denoted by the central cross in the figure and represents the muzzle pointing angle at the instant of projectile launch. The second vector indicates the deflection due to the velocity of the gun tube perpendicular to the line of flight (i.e. ratio of transverse muzzle velocity and projectile forward velocity).

Six orthogonal x-ray stations are located just downrange of the muzzle. The first three stations are placed close to the muzzle and observe the projectile just after it exits the muzzle and during the initial stages of the sabot discard process. The photographic data obtained from these x-rays provides both the initial yawing rates and linear c.g. motion of the projectile as it is launched. The deviation of the linear c.g. motion of the projectile from the pre-shot line of fire is represented on the closure diagram by the point which is marked "1" x-ray". The dashed line between the end of the gun dynamics vector and this point represents the sum of the disturbances caused by in-bore balloting motion, projectile "tip-off" or interaction between the gun tube and bullet as it exits the cannon, muzzle blast and the initial stages of the physical disengagement of the sabot from the subprojectile. This series of disturbances will be referred to as the mechanical disengagement phase.

The second three orthogonal x-ray stations are located further downrange, after the sabot has completely separated and the projectile has entered free flight. The angular deviation of the projectile c.g. motion obtained from these x-rays is represented in the

diagram by the point which is marked "2nd x-ray". The disturbance represented by the difference in the projectile trajectory measured by the two groups of x-rays is due to asymmetric sabot discard. The final two vectors in the diagram are the aerodynamic jump and gravity drop of the projectile.

After launch, the projectile flies through the BRL Transonic Range where it is photographed at 25 orthogonal spark shadowgraph stations covering 208 meters of the trajectory. The position and attitude of the projectile in time is defined from this data and forms the basis for the determination of both aerodynamic and trajectory characteristics. The trajectory provides a redundant measurement of properties near the gun and at the target. By extrapolating back toward the weapon, the Transonic Range data fit provides a verification of the x-ray data. Extrapolation downrange provides a check on the target impact information.

In the following few sections, each of the measurement techniques used in the analysis will be briefly discussed. Data obtained for the flight of a sabot cone stabilized training projectile (TPCSDS-T) will be used to illustrate both the measurement techniques and the closure analysis.

III. Gun Dynamics

While the in-bore time for a bullet is relatively short, the forces and moments exerted upon the gun tube by the high pressure combustion gases and the projectile are sufficient to cause a significant transverse motion of the tube prior to shot exit. This motion is due to the rotation of the gun about its support bearing and to the elastic vibration of the tube as it reacts to both the high pressure propellant gases and interacts with the projectile.

In previous gun dynamics investigations, a variety of experimental techniques have been utilized, including: optical methods,³ inductive transducers⁴ and strain gauges.⁵ The method employed in the current measurements is a refinement of the technique utilized by Biele⁶ in his investigation of the gun dynamics of the 120mm main gun of the West German Leopard II tank. The technique treats the gun tube as an elastic beam with an annular cross-section and utilizes a combination of strain gauges and proximity probes to determine the dynamic shape of the tube. The longitudinal bending strain of the tube, obtained from strain gauges mounted along the length of the gun, is proportional to the radius of curvature. For the small values of strain occurring during these tests

$$\epsilon = \frac{D}{2} \frac{d^2y}{dz^2} \quad (1)$$

³Gay, H.P. and Elder, A.S., "The Lateral Motion of a Tank Gun and its Effect on the Accuracy of Fire", Ballistic Research Lab Report 1070, U.S. Army Ballistic Research Laboratory, Aberdeen Proving Ground, MD 21005-3086, 1959

⁴Schmidt, J.Q. and Andrews, T.D., "Description of the Joint BRL-RARDE 40mm Experiment to Define Projectile Launch", in the Proceedings of the Fourth U.S. Army Symposium on Gun Dynamics, T.W. Simkins and J. Vasilakis (eds), Benet Weapons Laboratory, Watervliet NY 12189, 1985

⁵Simkins, T.E., Scanlon, R.D. and Benedict, R., "Transverse Motion of an Elastic Supported 30mm Gun Tube During Firing," Proceedings of the Third U.S. Army Symposium on Gun Dynamics, Rensselaerville, NY, May 1982

⁶Biele, J.K., "The Relationship of Gun Dynamics to Accuracy in a 120 mm Tank Gun", in the Proceedings of the 8th International Symposium on Ballistics, ADPA, 1984

where ϵ is the longitudinal bending strain, D is the outer diameter of the tube, z the axial coordinate along the length of the gun and y the coordinate perpendicular to the tube centerline. Integrating this expression twice yields the deflection of the tube as a function of z . Two constants of integration which can be obtained from an independent measurement of tube deflection are required to complete the computation. For these tests, eddy current proximity probes have been utilized to perform the displacement measurements. Although the technique requires that displacement measurements be made at only two locations, they have generally been performed at three or more locations during the current implementation. This redundancy has been utilized as a consistency check for the validity of the results. In the following two sections both the strain and displacement measurement techniques will be discussed.

1. Proximity Probes

The proximity gauges employed in these tests are commercially available units (Scientific-Atlanta model M-61 eddy probes coupled to model 606 eddy probe drivers) originally intended for use with rotating and reciprocating machinery. These small (diameter: 5 mm, length: 35 mm) transducers consist of an inductive element potted in an epoxy material. A high frequency electric current is passed through the device creating a magnetic field. When the transducer is in close proximity to a conducting surface (e.g. a steel gun tube), eddy currents are induced in the metal. The resulting loss of energy from the transducer is proportional to the gap between the unit and the surface and is a function of the material properties of the surface. Since the transducers were calibrated on the gun tube surface (i.e., the same type of metal was used for both calibration and during measurement), a time history of the current drawn by the probe is a direct measure of the gap between the transducer and the gun tube during the test.

It has been assumed that during the firing sequence, the cannon will undergo transverse motion in both the vertical (y) and horizontal (x) directions, recoil along the central axis (z) and radially expand or contract. It is also presumed that the cross section of the gun tube will remain circular. The outer surface of the tube can, however, be tapered. Under these conditions a minimum of three transducers are required to completely determine the translation and radial expansion of the gun at any position along its length. However, to simplify the data analysis, four transducers spaced 90 degrees apart around the circumference of the tube were utilized. In this configuration, the difference in the change of the gap width measured by two opposing probes will yield the translation of the gun along the axis joining the probes. The sum of the change in the gap widths, when corrected for the effect of tube taper and motion of the gun perpendicular to the probe axis yields the change in the diameter of the tube. A complete discussion of the application of proximity probes for gun dynamics measurements, including a discussion of system errors, can be found in Bornstein & Haug.⁷

Probes were placed at four locations along the tube as shown in figure 3: at two points in the vicinity of the muzzle (permitting the estimation of the muzzle pointing angle), near

⁷Bornstein, J. A. and Haug, H. T., "Gun Dynamics Measurements for Tank Gun Systems", BRL Memorandum Report MR-3688, U.S. Army Ballistic Research Laboratory, Aberdeen Proving Ground, MD 21005-5066, 1988

the center of the tube just forward of the bore evacuator and towards the rear portion of the tube near the thrust nut. To accommodate the strain gauges which were mounted on the tube, the probes were mounted along perpendicular axes oriented at 45 degrees to the vertical and horizontal directions. Data were acquired using transient recorders possessing a pre-trigger sampling capability. The instrumentation trigger signal was provided by a static pressure probe placed in close proximity to the muzzle (approximately 1 cm to the rear) that started the sampling process when the main blast wave associated with the high pressure propellant gases reached the pressure probe.

Figure 4 presents the translation of the tube measured by the four proximity probes situated near the muzzle while firing a sabot training round. A number of features are apparent in the figure. Notably, the lack of any significant motion of the muzzle prior to three milliseconds before shot exit, a spiral-like movement of the tube during the following 2.5 ms and finally a rapid motion of the tube both downwards and towards the right during the final few hundred microseconds before the projectile exits the gun.

Figure 5 displays the change in the outer diameter of the gun tube measured by the proximity probes. The passage of the projectile past the probe location is marked by a rapid expansion of the gun tube as the tube is suddenly subjected to high pressure, high temperature combustion gases in the bore of the tube. Since we anticipate that the expansion will be radial in nature, it is not surprising that the expansion measured along perpendicular axes is virtually identical. A by-product of the muzzle proximity probe measurements is a coarse estimate of the projectile velocity obtained by comparing the bullet passage times at two closely spaced axial locations.

The relative motion at the two locations close to the muzzle permit an estimate of the muzzle pointing angle as a function of time (figure 6). Inherent in this estimate is the assumption that the curvature of the tube between the measurement point and the muzzle is negligibly small; a criterion which cannot always be met. For these tests, however, the curvature in the vicinity of the muzzle was small and the proximity probes yield a good estimate of the pointing angle.

2. Strain Measurements

While the muzzle data are quite valuable, a description of the complete tube motion during the launch cycle permits a more detailed analysis of the projectile and gun tube interaction. To define the dynamic tube shape, strain gauges were mounted at eight axial stations along the gun (figure 3). Each station consisted of four orthogonal gauges (two each in the vertical and horizontal planes) oriented lengthwise along the tube. Diametrically opposed gauges were wired in a difference mode in the bridge completion circuits to reduce common mode signals such as hoop or pure axial stresses and to maximize the sensitivity to longitudinal bending strain. Data were initially multiplexed and recorded on analog tape. It was later played back and digitized, with the resulting information transferred to a digital computer for analysis. A sample strain data record (the raw data is marked "unfiltered") is shown in figure 7.

The analysis, developed by Heaps⁸ based upon the work of Biele, treats the gun tube as a cylindrical elastic beam which can deflect only due to longitudinal bending or rigid body motion. The longitudinal bending strain is related to the local curvature of the tube as shown in equation (1). Performing a double spatial integration of this expression yields the displacement due to the bending or the instantaneous shape of the tube. The two constants of integration are evaluated using the tube displacements obtained from proximity probes mounted near the muzzle and rear of the gun tube.

Sampling theory requires that the interval between successive data points be no larger than half the shortest wavelength of the signal (i.e. mode shape) to be measured. If shorter wavelengths (or higher modes) are present, aliasing will occur. In the current set of measurements, bending strain has been determined at 9 points on the tube (8 measurements and a zero strain condition at the muzzle), implying that at best we can hope to faithfully represent the shape of the tube through a linear combination of the first four vibration modes. This argument requires the employment of an anti-aliasing low pass filter with a cutoff frequency of 400 Hz. A sample of the filtered data is also shown in figure 7. Once the strain data were filtered, the data at any instant of time could be approximated by a polynomial function. The resulting function was then integrated twice and the proximity probe data were used to evaluate the two constants of integration. A more detailed discussion of the data analysis procedure can be found in Bornstein & Haug⁷.

Figure 8 depicts the results of the analysis, presenting both the vertical and horizontal shapes of the segment of the gun tube external to the turret during the in-bore period of the projectile, from 2.5 milliseconds prior to shot exit until the bullet is launched, at 500 microsecond intervals. The solid circles denote the location of the projectile at any instant of time, while the x's represent the proximity probe data used to obtain the constants of integration. Prior to -2.5 ms, the cannon exhibits little movement. The motion of the gun in the vertical plane is significantly larger than that observed in the horizontal plane. A wave-like whipping motion of the tube is apparent from the observation of successive frames in the plot. In the horizontal plane, the gun is constrained by the recoil system and is subject to motion which is more limited in amplitude. The driving force for this motion is presumably interaction between the projectile and gun tube.

The muzzle pointing angle can be obtained from these plots by numerically differentiating the displacement curve in the vicinity of the muzzle. The muzzle crossing velocity can be obtained by determining the rate of change of muzzle displacement at shot exit.

IV. Transitional Ballistics

The purpose of this portion of the test is to provide the bridge between the in-bore and the free flight dynamics of the projectile. Specifically, the motion of the projectile is recorded by flash radiography covering the region from the weapon muzzle through initial entry into undisturbed free flight, a distance of approximately 12 meters. A schematic representation of the x-ray set-up is given in figure 2. Six orthogonal x-ray units are

⁸Heaps, C.W., "Determination of Gun Tube Motion from Strain Measurements," BRL Memorandum Report BRL-MR-3562, U.S. Army Ballistic Research Laboratory, Aberdeen Proving Ground, MD 21005-5066, 1987

positioned in two groups of three each. The first group is placed in close proximity to the muzzle and captures the initial projectile position and orientation with respect to the line of fire. The second group is positioned further downrange, after the sabot separation process has occurred, and determines the linear and yawing motion as it enters free flight.

Six orthogonal Hewlett Packard 150 kV flash x-ray units are utilized to determine the transitional ballistics. Plywood cassettes protect the Kodak XAR840 X-Omat x-ray film which is exposed by Dupont Cronex Intensifying Screens bonded to the inner cassette surfaces. Both cassettes and x-ray heads are placed at a distance of approximately 1.5 meters from the line of fire. This provides sufficient source to object distance for a single head to completely illuminate the projectile and enough object to cassette distance to prevent reflected shock waves from disturbing the cassette before the x-ray of the projectile flight is recorded.⁹ During the test, the x-rays are fired sequentially, with the delay time between successive stations determined by the separation distance and the projectile muzzle velocity. The initial trigger signal for the entire system is provided by the muzzle pressure probe used for the gun dynamics measurements.

The standard calibration procedure for radiographs¹⁰ uses a double exposure technique. A fiducial cable is strung through the x-ray field of view close to the projectile line of flight (figure 9). The x-rays are pulsed at a low power level, the cable removed and the shot fired. The second, high power x-ray pulse places the image of the projectile on the same photograph. A sighting target is placed at the far end of the x-ray array, roughly 13 meters from the muzzle. The muzzle boresight aligns this target to the sight line. The boresight is removed and a second target is placed in the muzzle of the gun essentially locating the bore center line. The fiducial cable is strung between these two targets taking care that the cable does not touch the targets and distort their orientation. The cable contains both fiducial beads and two sightline spheres located near the target centers. The positions of these reference markers are located in the Transonic Range coordinate system using standard surveying techniques. The downrange target is then removed and the x-rays pulsed at a low power level. Since both reference spheres appear on the x-ray photographs, the sight line is also captured. The fiducial cable is then removed and the round fired. The calibration procedure ensures that the fiducial cable lies along the line of fire and permits a straightforward evaluation of the projectile linear and angular position. The cable survey also locates the line of fire permitting a determination of the variation in jump through the x-ray rig.

Figure 10 is a set of orthogonal views of a cone stabilized, discarding sabot training projectile as it is launched from the gun tube. In the figure, the upper photograph corresponds to a view of the projectile taken from below, while the lower image is a side view of the bullet. Immediately after disengagement from the gun tube, the sabot components remain essentially in the as-fired position. In this example, the cone base of the projectile is just clearing the muzzle. The recoiling motion of the muzzle can also be observed, with the fainter image of the muzzle corresponding to its position prior to the test and the more intense image corresponding to the muzzle as the projectile exits the gun. Also visible in

⁹Schmidt, E.M., Plostins, P. & Bundy, M.L., "Flash Radiographic Diagnostics of Projectile Launch," in the Proceedings of the 1984 Flash Radiography Symposium, E.A. Webster, Jr. & A.M. Kennedy (eds), The American Society for Nondestructive Testing, 4135 Arlingate Plaza, Columbus OH 43221, 1984

¹⁰Schmidt, E.M. & Shear, D.D., "Aerodynamic Interference during Sabot Discard," USABRL Report R-2019, U.S. Army Ballistic Research Laboratory, Aberdeen Proving Ground, MD, 21005-5066, 1977

the photo are the fiducial cable and the two reference beads for this station. As part of the calibration procedure, the distance between the notches in each of the beads is measured. Comparison of this distance, with the distance between these two points in the x-ray image yields an in-situ determination of the magnification factor for each x-ray, eliminating the necessity to accurately measure the distance between each head and the object and film planes.

Just downrange of the muzzle (figure 11), the components begin to rotate off the flight body. Contact is maintained between the aft end of the sabot and the projectile up to the third x-ray station. In the illustration, one of the sabot petals has already lifted off at the rear, an excellent example of a discard asymmetry. In the side view shown in figure 11, one can also see a significant pitch angle between the projectile and the fiducial cable developing. Between the third and fourth stations, the components lift away and only aerodynamic interaction continues. By the time the projectile reaches the second set of three x-ray stations, the sabot components are still within the x-ray field of view, but have moved sufficiently far from the flight body to preclude further interaction and the projectile is in undisturbed free flight (figure 12).

The motion of the center of gravity of a sabot projectile through the x-ray system is presented in figures 13 and 14, together with the measured line of fire. In the figures, the z axis corresponds to the downrange coordinate, while the y and x axes correspond to the vertical and horizontal coordinates respectively. The plot of the projectile vertical motion shows that the projectile begins its trajectory at a point in space near the static muzzle location but with a "separation angle" above the line of fire. This angle is a component of the total jump representing the sum of all perturbations seen by the projectile up to this point in the trajectory, including: tank, gun tube, mechanical discard, muzzle blast and initial sabot discard disturbances. During passage of the bullet through the location of the first three x-ray stations, the projectile does not appear to be subjected to any significant accelerations and its trajectory can be approximated by a straight line. In the horizontal plane (fig 14), the projectile is to the right of the line of fire; the trajectory again is at a small angle with respect to the line of fire. Due to the smaller deflection in the horizontal plane, errors in the determination of the projectile center of gravity are more apparent in this plot. The scale of these errors is of the order of "0.5 mm", which is the accuracy to which we expect to be able to read deflections on the x-ray. The c.g. trajectory is still approximated by a linear fit.

Between the first and last set of x-rays, the sabot discard process goes to completion. Further alterations to the trajectory may occur in this region leading to an "initial free flight departure angle." The differences in the muzzle separation and initial free flight departure angles are more apparent in the horizontal plane in this example, though this is by no means the rule.

To this point, the x-ray data has been utilized to consider the linear motion of the projectile. However, the contributions of launch dynamics to total jump are not completely defined until the aerodynamic jump (or jump due to yaw) has been treated. The angular motion of the projectile as a function of the downrange location is given in figures 15 and 16. The x-ray data show that the projectile is launched with a very small yaw angle, consistent with the strong constraints provided by the sabot components and the gun

tube. The round has a finite angular velocity about its center of gravity (or yaw rate) as it exits the cannon and the yaw angle grows accordingly. This is more apparent in the vertical plane, where the yaw angle has grown to approximately 1.25 degrees at the third x-ray station, than it is in the horizontal plane, where the yaw measured at the first three stations is less than 0.1 degree or roughly the order of the estimated accuracy (± 0.1 deg) that can be obtained from a good quality x-ray. In the figure, the squares represent the yaw angles determined from the x-rays, while the solid line is a prediction of the yawing motion of the projectile based on the measured angular rate in the first three x-ray stations (i.e. prior to sabot separation) and a knowledge of the aerodynamic coefficients for the projectile.

As the round moves through the sabot discard region, it is subjected to angular disturbances caused by asymmetries in the process. These cause a change in the yawing motion. The dashed curve represents the predicted free flight yaw behaviour based on the angular rate measured in x-ray stations 4 through 6. These yaw rates can be used to compute the projectile free flight aerodynamic jump². The solid curve represents the predicted angular motion of the projectile if it had entered free flight at the muzzle.

V. Jump Analysis

Figure 17 depicts the closure analysis, introduced in section 2, for a sabot cone stabilized training projectile. In this case, gravity drop has been accounted for by shifting the aim point. Looking first at the gun dynamics disturbance for this round, the muzzle pointing angle makes a significant contribution to the overall jump, providing a disturbance of approximately 0.45 mils in magnitude, while the contribution of the crossing velocity is much smaller, roughly 0.12 mils in magnitude. Experience gained firing a number of these rounds has shown that the round to round variation in the magnitude and orientation of both of these vectors was fairly small.

The trajectory of the projectile just after it has been launched but before sabot discard has occurred (determined from the first three x-ray stations) is represented by the point marked first x-ray. The effects of in-bore projectile motion, muzzle blast and tip-off disturbances have been lumped together into the vector which joins this point and the tip of the muzzle crossing velocity vector. The magnitude of this vector is comparable to the muzzle pointing angle. However the observed variation of both the magnitude and orientation of the vector was larger than for the gun dynamics. This was also found to be the case for the disturbance caused by the sabot discard process, which is represented by the vector joining the trajectories determined for the 1st and 2nd group of x-rays. Lastly, for this particular case the magnitude of the yawing motion was fairly small and the aerodynamic jump computed from the projectile angular velocity measured by the second group of x-rays (i.e. as the projectile enters into free flight) is similarly small. The tip of the vector representing aerodynamic jump is the angular coordinate for the expected impact point of the projectile, once the effect of gravity drop has been removed. As the figure indicates, the difference between this point and the actual impact is approximately 0.17 mils, within the 0.2 mil accuracy we attribute to the measurement techniques.

VI. Concluding Remarks

This paper has briefly discussed the methodology and measurement techniques which have been developed at BRL to quantitatively determine the contribution of individual disturbance sources to the overall jump of a projectile. The technique has been applied with success to both sabot and full-bore ammunition for the 105 mm M68A1 and 120 mm M256 Cannon used by the M1 and M1A1 tanks. Similar methods, on a smaller scale, are also currently being used to examine the performance of 25 mm ammunition.

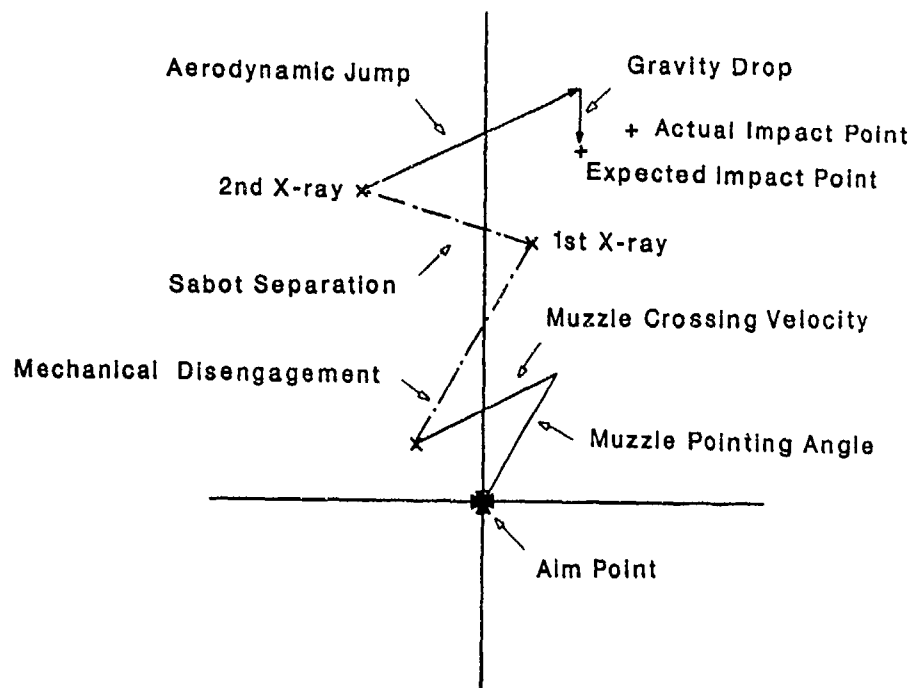


Figure 1. Vector diagram indicating the closure analysis with sources of disturbance to the projectile trajectory

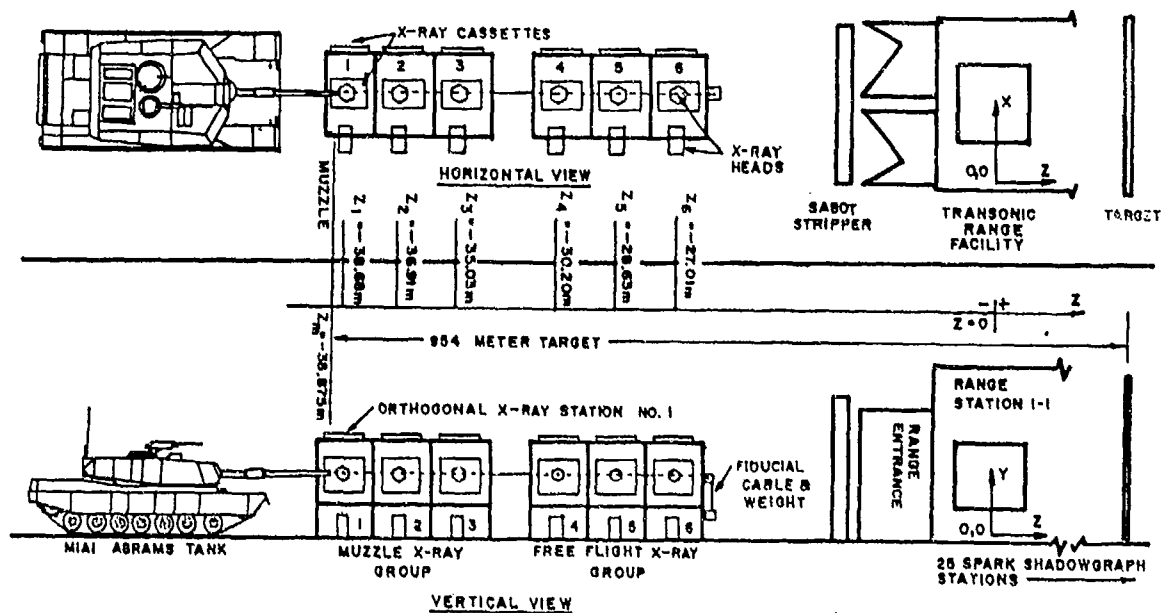


Figure 2. Schematic diagram of set-up for tests

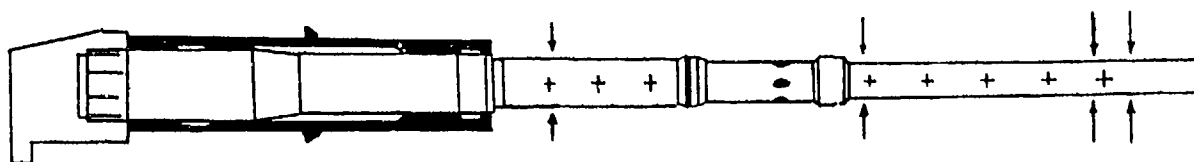


Figure 3. Diagram of 120mm M256 gun tube with breech indicating the location of the proximity probes (arrows) and strain gauges (crosses) used to determine the gun dynamics

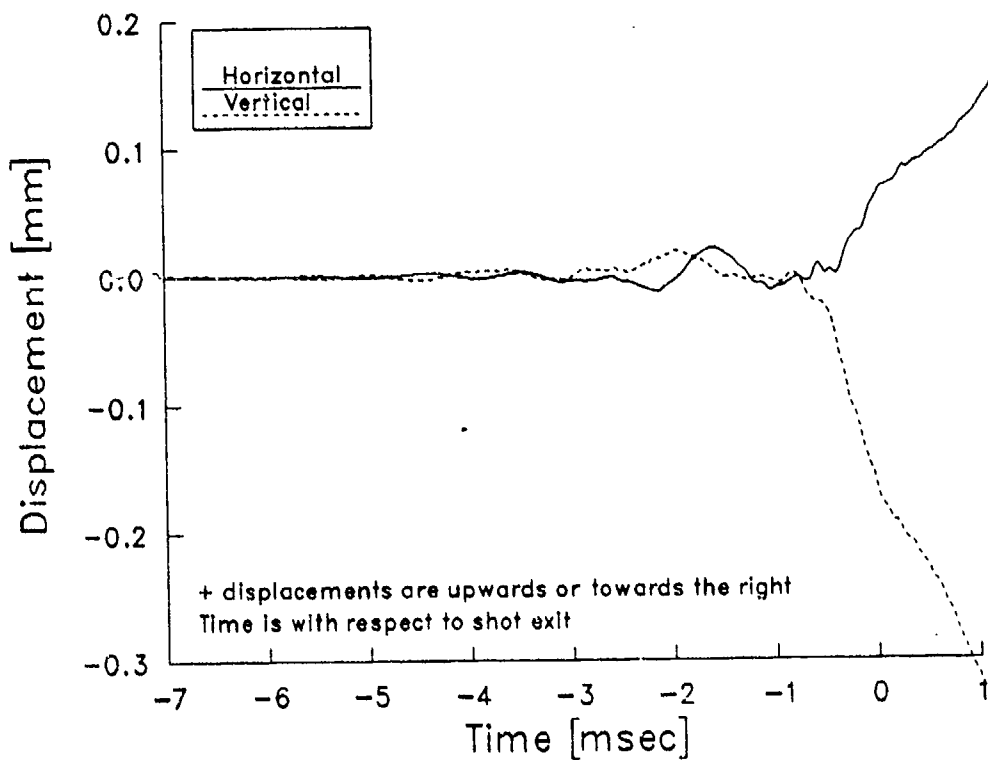


Figure 4. Transverse motion of the gun tube near the muzzle (TPCSDS-T projectile)

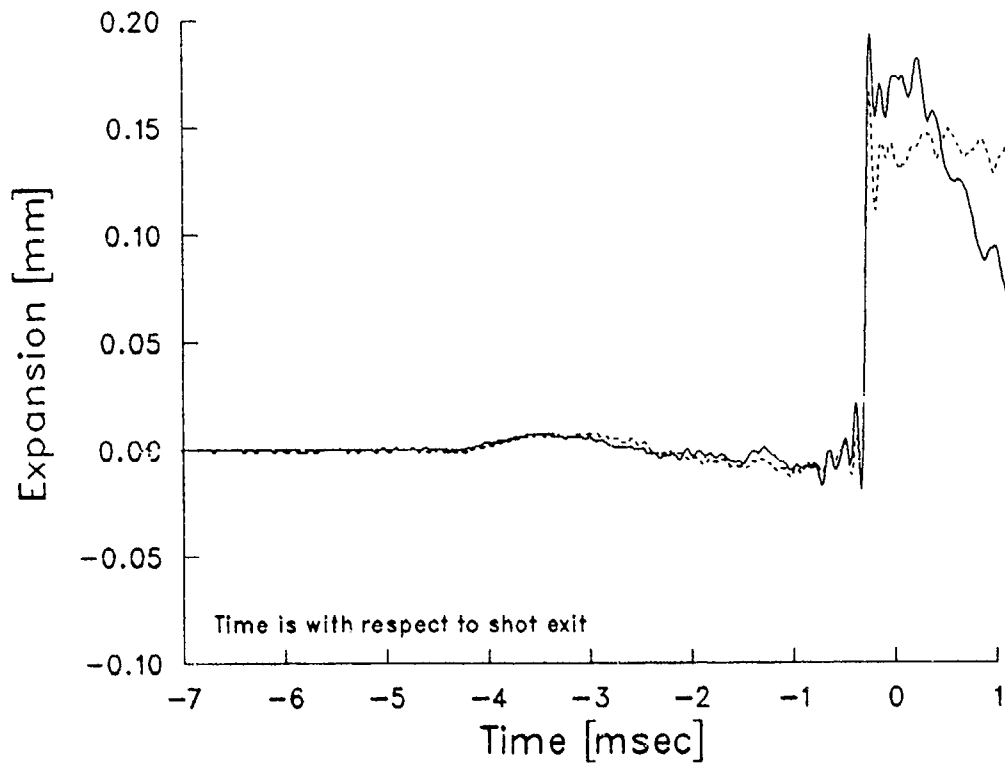


Figure 5. Expansion of the gun tube near the muzzle (TPCSDS-T projectile)

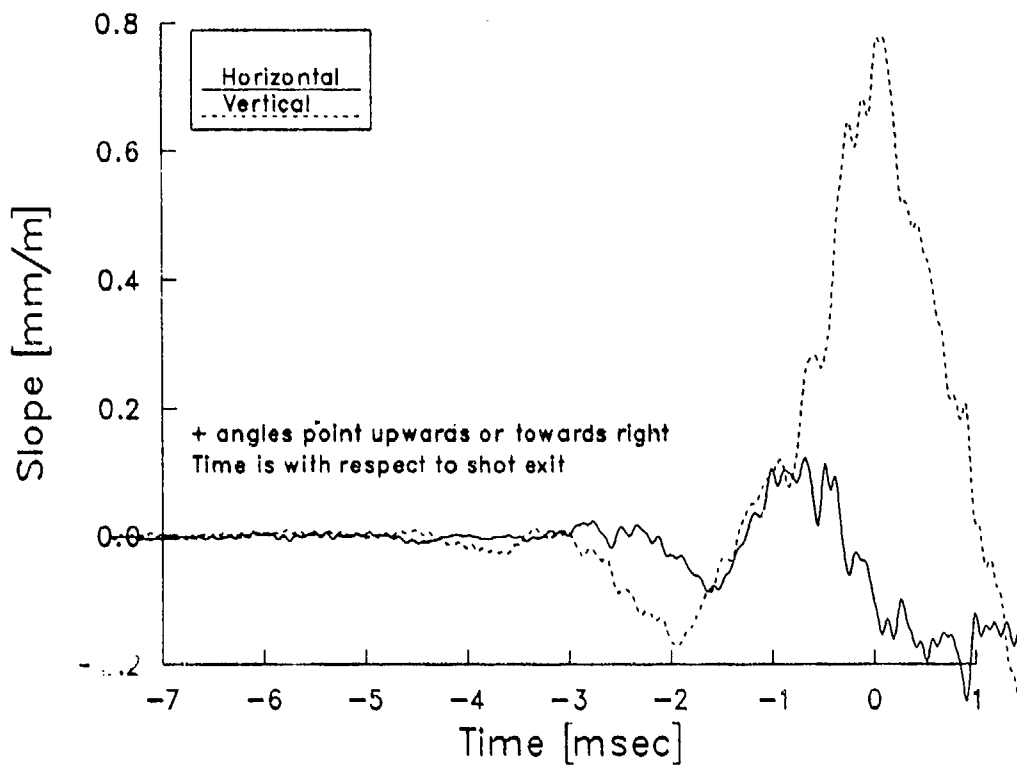


Figure 6. Muzzle pointing angle measured by proximity probes (TPCSDS-T projectile)

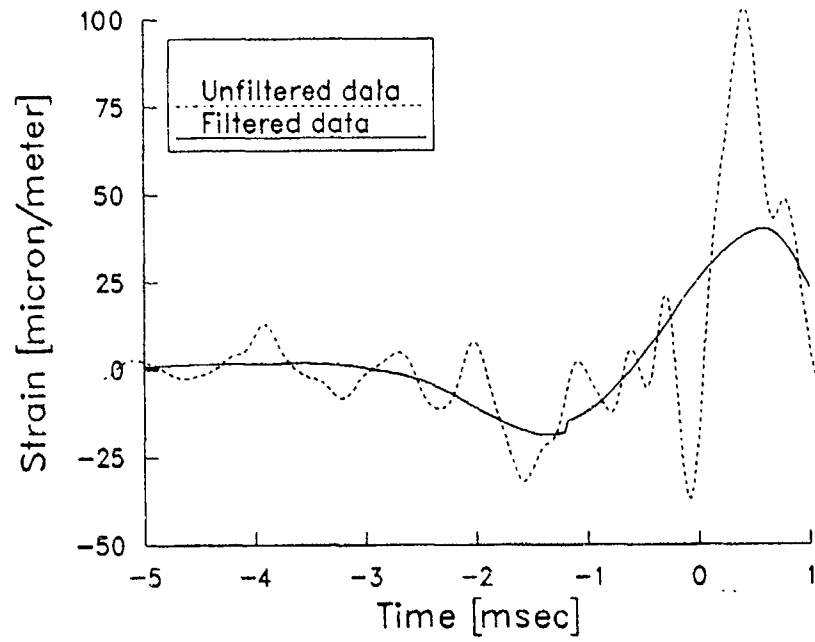


Figure 7. Sample strain record

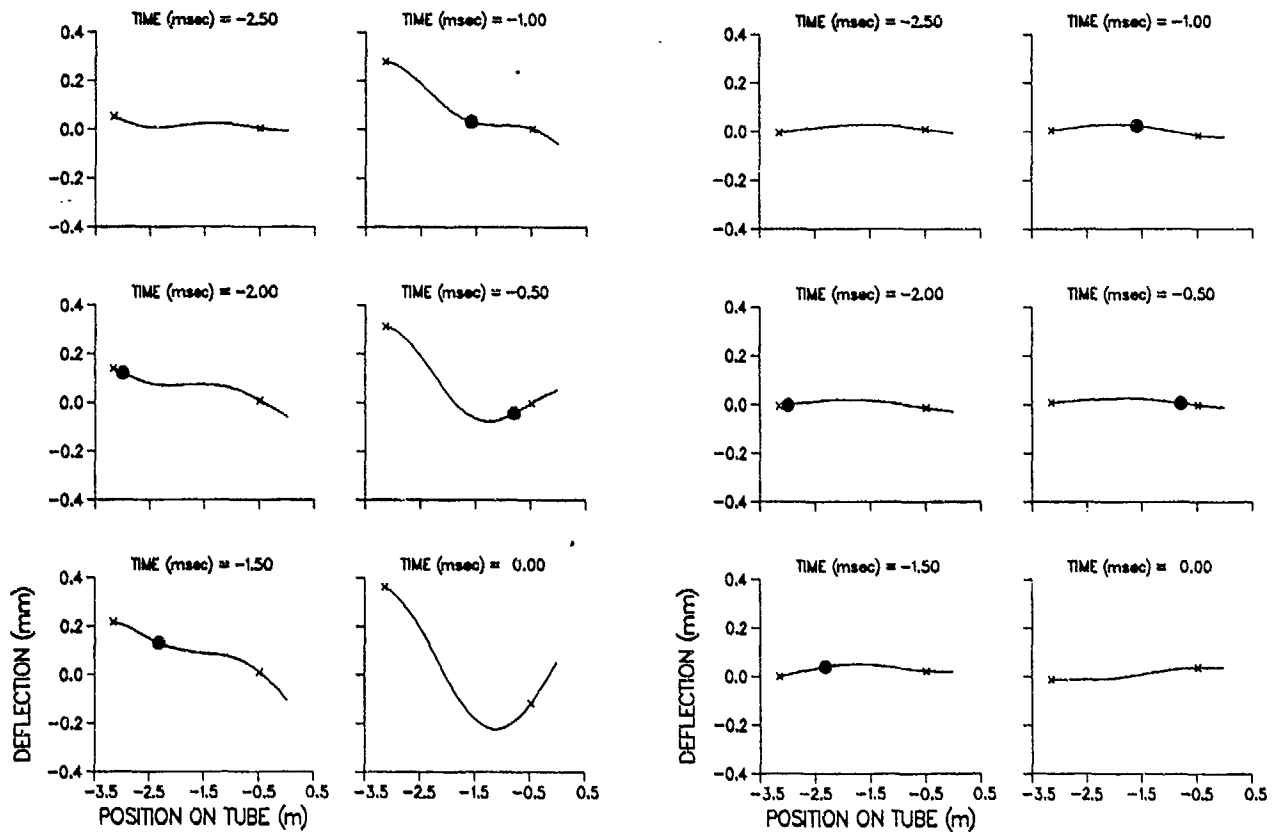


Figure 8. Displacement of the tube (a) vertical plane, (b) horizontal plane

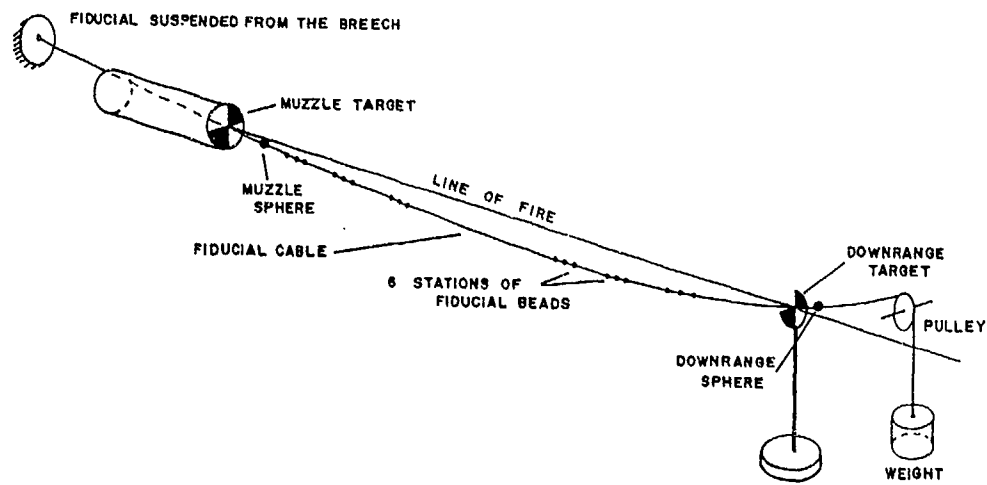


Figure 9. Schematic representation of x-ray set-up

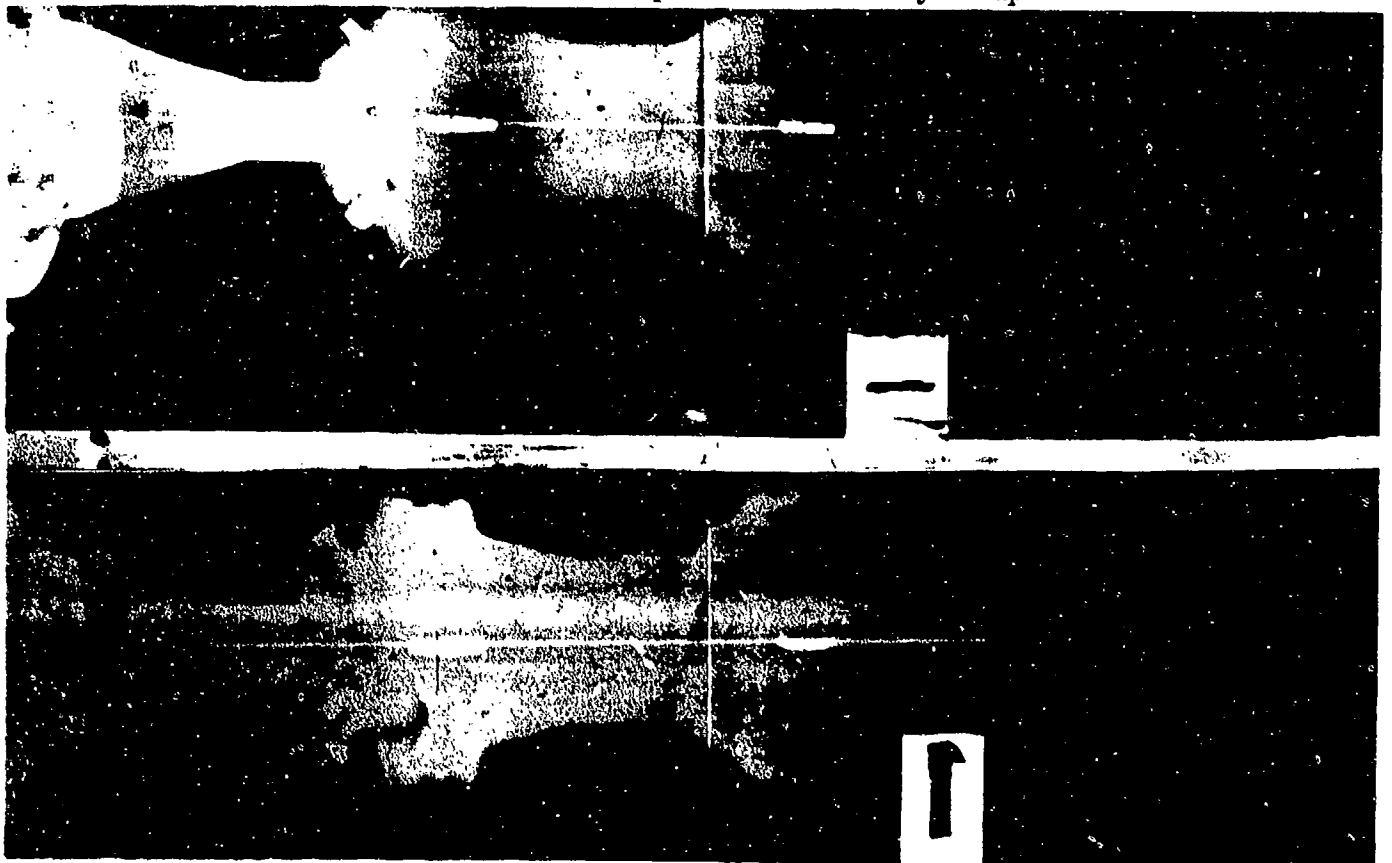


Figure 10. TPCSDS-T projectile at launch. Muzzle is shown at left of photo. Lower image shows pitching of projectile, upper indicates yawing motion

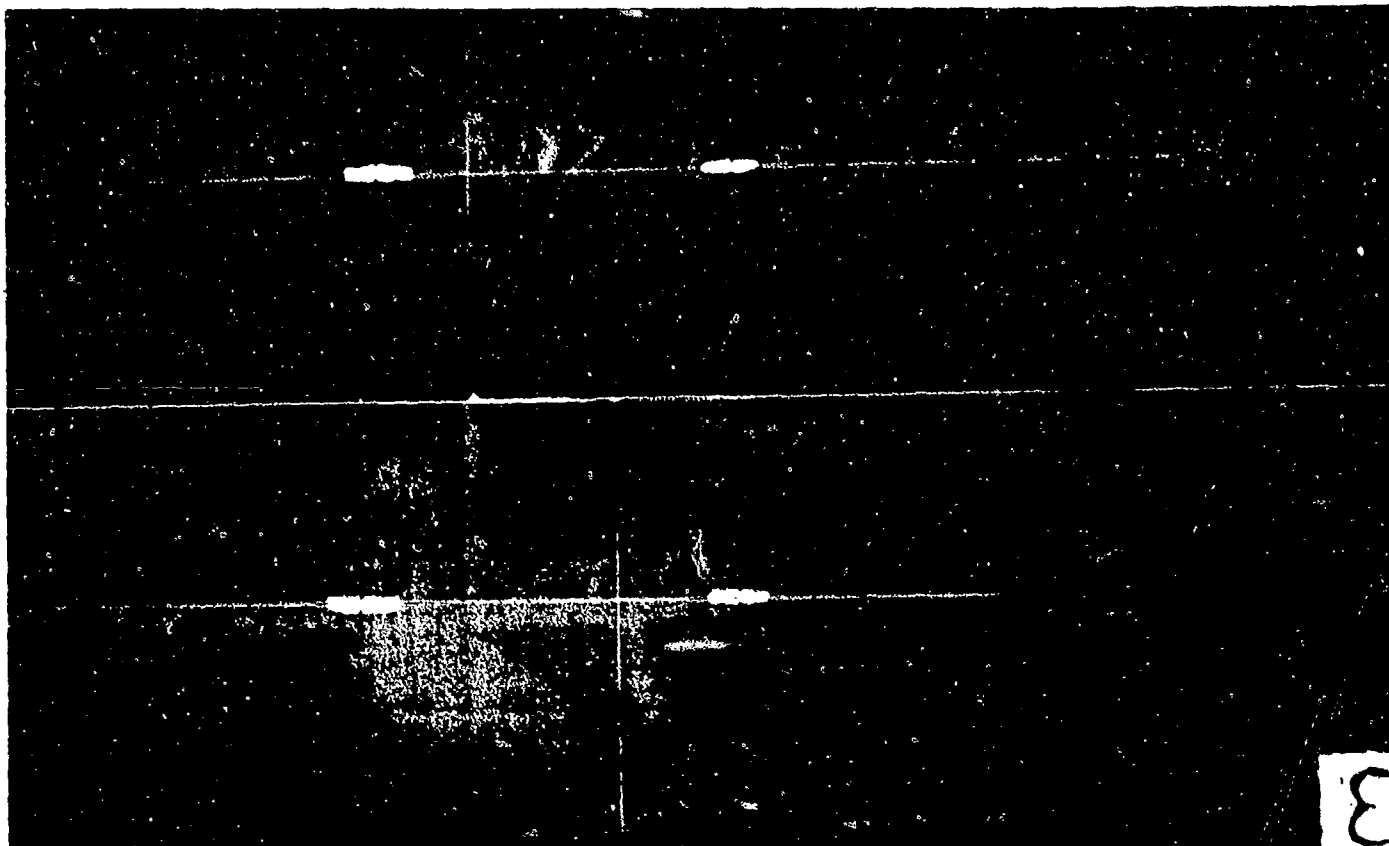


Figure 11. TPCSDS-T projectile 3 meters downrange of muzzle. Lower photo shows pitching of projectile, upper indicates yawing motion



Figure 12. TPCSDS-T projectile entering free flight, 10.4 meters downrange. Lower photo shows pitching of projectile, upper indicates yawing motion

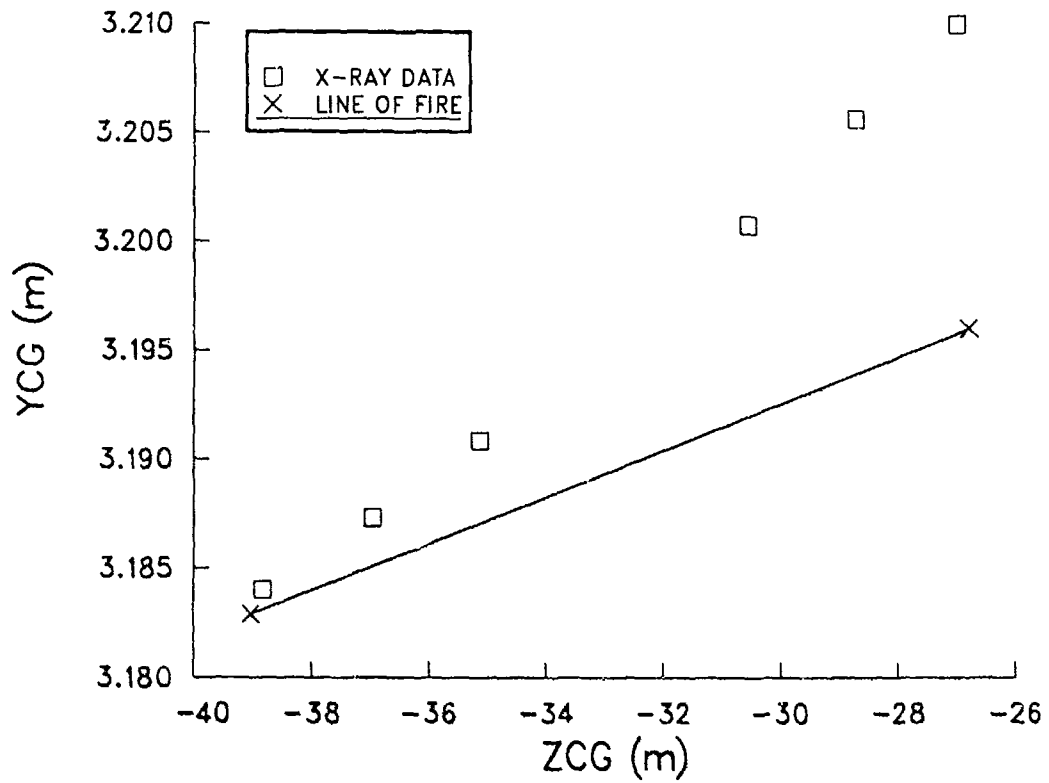


Figure 13. CG trajectory of TPCSDS-T projectile - vertical plane

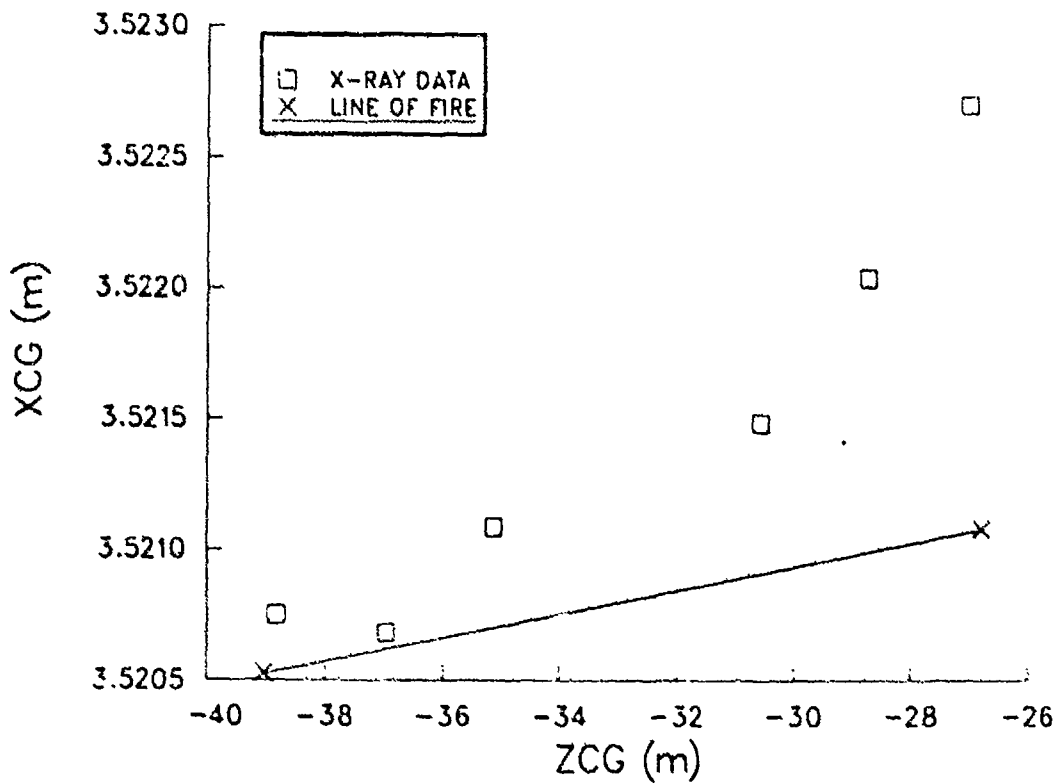


Figure 14. CG trajectory of TPCSDS-T projectile - horizontal plane

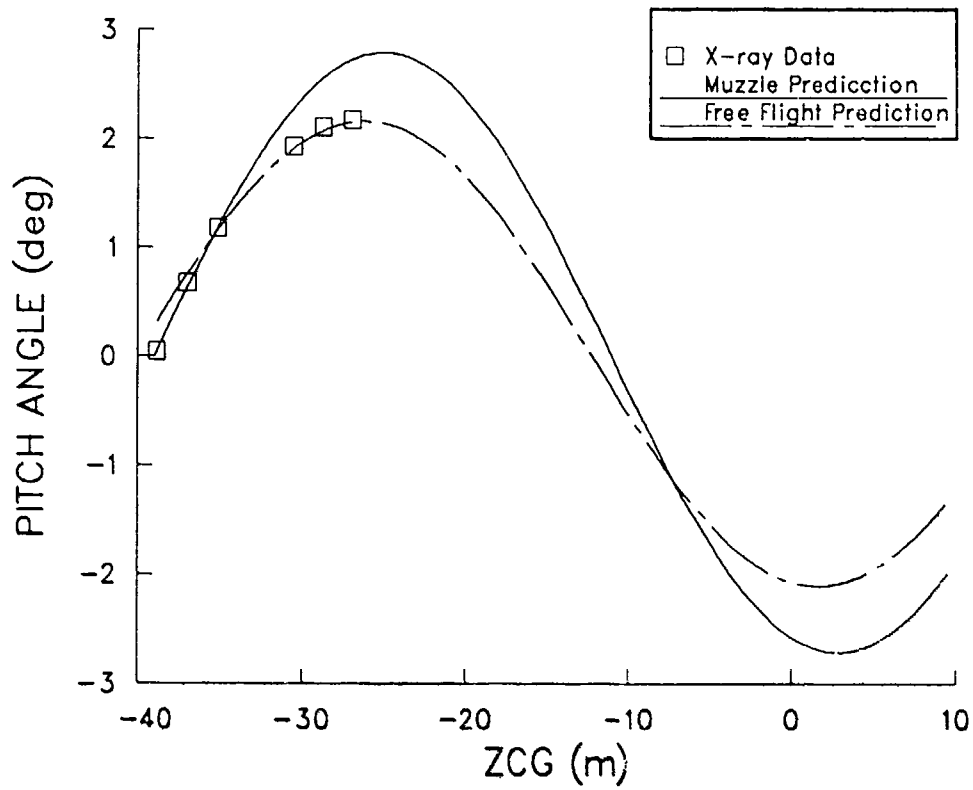


Figure 15. Pitch history for TPCSDS-T projectile determined from x-ray data

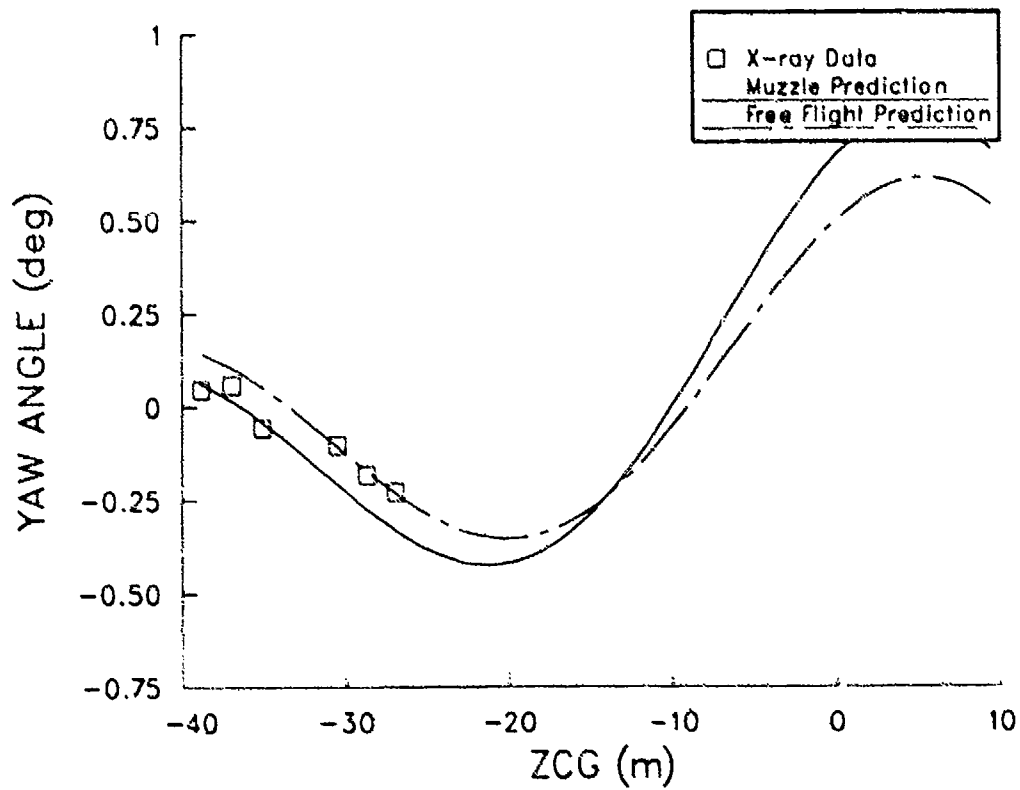


Figure 16. Yaw history for TPCSDS-T projectile determined from x-ray data

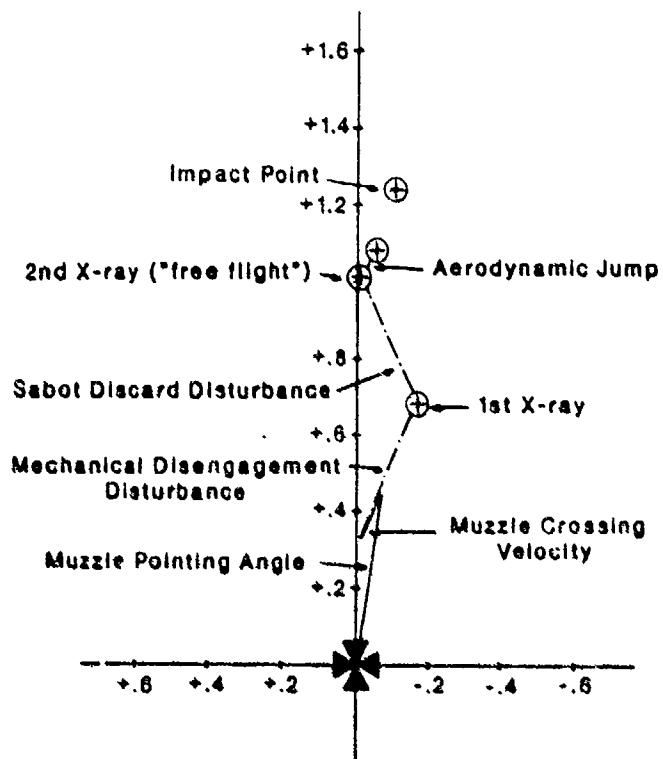


Figure 17. Closure diagram for TPCSDS-T projectile

VII. References

1. Plostins, P., "Launch Dynamics of APFSDS Ammunition," Technical Report BRL-TR-2595, U.S. Army Ballistic Research Laboratory, Aberdeen Proving Ground, MD 21005, 1984, AD# A147314
2. Murphy, C.H., "Free Flight Motion of Symmetric Missiles," BRL Technical Report 1216, U.S. Army Ballistic Research Laboratory, Aberdeen Proving Ground, MD 21005, 1963, AD# 442374
3. Gay H.P. and Elder A.S., "The Lateral Motion of a Tank Gun and its Effect on the Accuracy of Fire," Ballistic Research Lab Report 1070, U.S. Army Ballistic Research Laboratory, Aberdeen Proving Ground, MD 21005, 1959 AD# 217657
4. Schmidt J.Q. and Andrews T.D., "Description of the Joint BRL-RARDE 40mm Experiment to Assess Projectile Launch Parameter Measurement Techniques," BRL-TR-2679, U.S. Army Ballistic Research Laboratory, Aberdeen Proving Ground, MD 21005, Sept 1985, AD#B087033
5. Simkins T.E., Scanlon R.D. & Benedict R., "Transverse Motion of an Elastic Supported 30mm Gun Tube During Firing," in the Proceedings of the Third U.S. Army Symposium on Gun Dynamics, T.W. Simkins (ed), Benet Weapons Laboratory, Watervliet NY 12189, 1982, AD# B065338
6. Biele J.K., "The Relationship of Gun Dynamics to Accuracy in a 120 mm Tank Gun," in the proceedings of the 8th International Symposium on Ballistics, ADPA, 1984
7. Bornstein J.A. & Haug B.T., "Gun Dynamics Measurements for Tank Gun Systems," BRL Memorandum Report MR-3688, U.S. Army Ballistic Research Laboratory, Aberdeen Proving Ground, MD 21005-5066, July 1988 AD# B122913
8. Heaps C.W., "Determination of Gun Tube Motion from Strain Measurements," BRL Memorandum Report BRL-MR-3562, U.S. Army Ballistic Research Laboratory, Aberdeen Proving Ground, MD 21005, 1987, AD# B110660
9. Schmidt E.M., Plostins P. & Bundy M.L., "Flash Radiographic Diagnostics of Projectile Launch," in the proceeding of 1984 Flash Radiography Symposium, Webster E.A., Jr. & Kennedy A.M.(eds). The American Society for Nondestructive Testing, 4175 Arlingate Plaza, Columbus, OH 43221, 1984
10. Schmidt E.M. & Shear D.D., "Aerodynamic Interference during Sabot Discard," USABRL Report R-2019, U.S. Army Ballistic Research Laboratory, Aberdeen Proving Ground, MD 21005, 1977, AD# A53308

LIST OF SYMBOLS

C_L	Lift Coefficient $\frac{\text{Lift Force}}{\frac{1}{2}\rho V^2 S}$
C_M	Pitching Moment Coefficient $\frac{\text{Pitching Moment}}{\frac{1}{2}\rho V^2 S l}$
l	reference length
S	reference area (normally l^2)
V	Projectile velocity
ξ	yaw angle of projectile
ξ'	yaw rate of projectile

SUBSCRIPTS

α	derivative with respect to angle of attack
o	initial value

DISTRIBUTION LIST

<u>No. of Copies</u>	<u>Organization</u>	<u>No. of Copies</u>	<u>Organization</u>
12	Administrator Defense Technical Information Center ATTN: DTIC-DDA Cameron Station, Alexandria, VA 22304-6145	1	Commander US Army Armament, Munitions and Chemical Command ATTN: SMCAR-ESP-L Rock Island, IL 61299
1	HQDA (SARD-TR) Washington, DC 20310	1	Commander US Army Aviation Systems Command ATTN: AMSAV-DACL 4300 Goodfellow Blvd. St. Louis, MO 63120
1	Commander US Army Materiel Command ATTN: AMCDRA-ST 5001 Eisenhower Avenue Alexandria, VA 22333-0001	1	Director US Army Aviation Research and Technology Activity Ames Research Center Moffett Field, CA 94035-1099
1	Commander US Army Laboratory Command ATTN: AMSLC-TD Adelphi, MD 20783-1145	1	Commander US Army Communications - Electronics Command ATTN: AMSEL-ED Fort Monmouth, NJ 07703
1	Commander Armament R&D Center US Army AMCCOM ATTN: SMCAR-MSI Picatinny Arsenal, NJ 07806-5000	1	Commander US Army Missile Command ATTN: AMSMI-RD Redstone Arsenal, AL 35898-5000
1	Commander Armament R&D Center US Army AMCCOM ATTN: SMCAR-TDC Picatinny Arsenal, NJ 07806-5000	1	Commander US Army Missile Command ATTN: AMSMI-AS Redstone Arsenal, AL 35898-5500
1	Director Benet Weapons Laboratory Armament RD&E Center US Army AMCCOM ATTN: SMCAR-LCB-TL Watervliet, NY 12189	1	Commander US Army Tank Automotive Command ATTN: AMSTA-DI Warren, MI 48090

DISTRIBUTION LIST

<u>No. of Copies</u>	<u>Organization</u>	<u>No. of Copies</u>	<u>Organization</u>
1	Director US Army TRADOC Analysis Command ATTN: ATAA-SL White Sands Missile Range, NM 88002	2	President US Army Armor & Engineer Board ATTN: ATZK-AE-PD, Mr. A. Pomey Mr. W. Wells Fort Knox, KY 40121
1	Commandant US. Army Infantry School ATTN: ATSH-CD-CSO-OR Fort Benning, GA 31905	6	Commander US Army Tank Automotive Command ATTN: PM-M1A1, LTC Barbara LTC Kaye Mr. G. Howe Dr. M. Pattison
1	Commander US Army Research Office P.O. Box 12211 Research Triangle Park, NC 27709		ATTN: PM-M1 ATTN: PM-M60 Warren, MI 48090
1	Commander US Naval Air Systems Command ATTN: AIR-604 Washington, DC 20360	4	Commander Tank Main Armament Systems ATTN: AMCPM-TMA, R. Billington K. Russell V. Rosamillia E. Kopacz Dover, NJ 07801-5001
1	Commander US Army Development and Employment Agency ATTN: MODE-TED-SAB Ft. Lewis, WA 98433	10	Commander US Army Armament RD&E Center ATTN: SMCAR-FS, Dr. Davidson Mr. Garver Mr. Frauen ATTN: SMCAR-FSF, Mr. Ambrosini ATTN: SMCAR-FSA, Mr. Wrenn ATTN: SMCAR-CC, Mr. Hirshman Mr. Staton ATTN: SMCAR-CCH, Mr. Moore Mr. Barrieres ATTN: SMCAR-CCL, Mr. Gehbauer Dover, NJ 07801-5001
1	AFWL/SUL Kirtland AFB, NM 87117-6008		
1	Air Force Armament Laboratory ATTN: AFATL/DLODL Eglin AFB, FL 32542-5000		
1	Commandant USAFAS Fort Sill, OK 73503-5600		

DISTRIBUTION LIST

<u>No. of Copies</u>	<u>Organization</u>	<u>No. of Copies</u>	<u>Organization</u>
6	Director Benet Weapons Laboratory ATTN: SMCAR-CCB, L. Johnson T. Simkins T. Allen ATTN: SMCAR-LDB-D, J. Zweig ATTN: SMCAR-LCB-DS, P. Vottis R. Hasenbein 1 Watervliet, NY 12189	3	Honeywell Inc ATTN: G.L. Campbell C. Candland D. Magnes 7225 Northland Drive Brooklyn Park, MN 55428 Honeywell Ordnance ATTN: Craig Sletto Mail Stop 111443 23100 Sugarbush Road Elk River, MN 55330 AAI Corporation ATTN: J. Herbert P.O. Box 6767 Baltimore MD 21204
3	Commander US Army Watervliet Arsenal ATTN: SMCWV-QAR, T. McCloskey ATTN: SMCWV-ODW, T. Fitzpatrick 1 ATTN: SMCWV-ODP, G. Yarter Watervliet, NY 12189	1	Commander US Army Armor Center & School ATTN: ATSB-SMT, Maj Newlin Fort Knox, KY 40121
1	Commander US Army Armor Center & School ATTN: ATSB-SMT, Maj Newlin Fort Knox, KY 40121	2	Aerojet Ordnance Co ATTN: W. Wolterman S. Rush 2521 Michelle Drive Tustin, CA 92680
2	Olin Corporation ATTN: L.A. Mason D. Marlowe 707 Berkshire Blvd East Alton, IL 62024	1	Princeton Scientific Instruments, Inc ATTN: John Lowrance P.O. Box 252 Kingston, NJ 08528
3	Honeywell Inc ATTN: R. Gartner G. Stillely R. Kenyon 10400 Yellow Circle Drive Minnetonka, MN 55343		

Aberdeen Proving Ground

Director, USAMSAA
ATTN: AMXSY-D
ATTN: AMXSY-D, Mr. W. Brooks
Mr. B. Siegel
Mr. R. Conroy
ATTN: AMXSY-MP, Mr. H. Cohen

Commander, USATECOM
ATTN: AMSTE-TO-F

Commander, USACSTA
ATTN: STECS-AV-T, Mr. W. Swank
ATTN: STECS-AS-HT, Mr. H. Zelik
Mr. H. Greuter
ATTN: STECS-CC-PF, Mr. P. McCall

Commander, USATECOM
ATTN: AMSTE-TE-R, Mr. Keele
ATTN: AMSTE-CM-R, Mr. Saubier

Commander, CRDEC, AMCCOM
ATTN: SMCCR-RSP-A
ATTN: SMCCR-MU
ATTN: SMCCR-SPS-IL

USER EVALUATION SHEET/CHANGE OF ADDRESS

This Laboratory undertakes a continuing effort to improve the quality of the reports it publishes. Your comments/answers to the items/questions below will aid us in our efforts.

1. BRL Report Number _____ Date of Report _____

2. Date Report Received _____

3. Does this report satisfy a need? (Comment on purpose, related project, or other area of interest for which the report will be used.) _____

4. How specifically, is the report being used? (Information source, design data, procedure, source of ideas, etc.) _____

5. Has the information in this report led to any quantitative savings as far as man-hours or dollars saved, operating costs avoided or efficiencies achieved, etc? If so, please elaborate. _____

6. General Comments. What do you think should be changed to improve future reports? (Indicate changes to organization, technical content, format, etc.) _____

CURRENT ADDRESS

Name _____
Organization _____
Address _____
City, State, Zip _____

7. If indicating a Change of Address or Address Correction, please provide the New or Correct Address in Block 6 above and the Old or Incorrect address below.

OLD ADDRESS

Name _____
Organization _____
Address _____
City, State, Zip _____

(Remove this sheet, fold as indicated, staple or tape closed, and mail.)